Analyzing Glide-Symmetric Holey Metasurfaces Using a Generalized Floquet Theorem

Fatemeh Ghasemifard, Martin Norgren, Oscar Quevedo-Teruel, Guido Valerio

IEEE Access
Multidisciplinary | Rapid Review | Open Access Journal

Received September 4, 2018, accepted November 6, 2018, date of publication November 19, 2018,
date of current version December 18, 2018.

Digital Object Identifier 10.1109/ACCESS.2018.2882056

Analyzing Glide-Symmetric Holey Metasurfaces Using a Generalized Floquet Theorem

FATEMEH GHASEMIFARD[1], (Graduate Student Member, IEEE), MARTIN NORGREN[1], (Member, IEEE), OSCAR QUEVEDO-TERUEL[1], (Senior Member, IEEE), AND GUIDO VALERIO[2], (Senior Member, IEEE)

[1]Department of Electromagnetic Engineering, School of Electrical Engineering and Computer Science, KTH Royal Institute of Technology, 114 28 Stockholm, Sweden
[2]Laboratoire d'Electronique et Electromagnetisme, Sorbonne Université, 75252 Paris, France

Corresponding author: Fatemeh Ghasemifard (fatemehg@kth.se)

This work was supported in part by the Swedish STINT Postdoctoral Transition Grants programme under Grant PT2014-5813 funded by the Swedish Foundation for International Cooperation in Research and Higher Education and in part by the French ANR under Grant HOLeYMETA ANR-16-CE24-0030.

ABSTRACT In this paper, we present a general mode matching formulation to analyze the wave propagation in glide-symmetric metallic surfaces drilled with periodic holes with an arbitrary cross section. A generalized Floquet theorem is applied to reduce the computational cost by imposing boundary conditions only on one of the two surfaces. With a small modification, the formulation can be used also for dispersion analysis of a holey metallic surface with or without a metal plane above it. The method is fast and efficient, and it provides physical insight on the specific symmetry properties of Floquet harmonics in glide-symmetric structures. The formulation is applied to obtain dispersion diagrams of glide-symmetric structures with circular holes as this kind of hole is usually used in practical applications to realize gap waveguides or wideband planar lenses. The results agree well with the reference results from commercial software *CST Microwave Studio*.

INDEX TERMS Dispersive analyses, generalized Floquet theorem, glide symmetry, higher symmetries, metasurfaces, mode matching, periodic structures.

I. INTRODUCTION

The emergence of metasurfaces has inspired new antenna applications and technological solutions [1], [2]. Metasurfaces provide the possibility of realizing graded-index lenses [3], [4] and creating stop-bands to prevent the propagation acting as electromagnetic band gap (EBG) structures. For example, the latter metasurfaces are used to implement gap waveguide technology, which has application in low-loss high frequency microwave components and antennas [5], [6].

Graded-index metasurface lens antennas typically have a narrow frequency bandwidth. Recently, it has been demonstrated that by applying higher symmetries such as glide [7]–[10], twist [11], [12] and polar-glide [13], [14] to periodic structures, the frequency dispersion of the first propagating mode is reduced. This technique offers the possibility of designing wideband lens antennas [15]–[17]. These antennas find application in 5G communications systems [18], [19]. Moreover, glide-symmetric holey structures have been proposed to produce low-cost and broad-band EBG structures that can be used in designing waveguiding structures [20], [21], flanges [22], and microwave components [23] at millimeter-waves.

One-dimensional high-symmetric periodic structures were first studied in the 1960s and 1970s [24]–[26] in connection to the theory of periodic waveguides. In 1973, a generalized Floquet theorem was proposed to explain the wave distribution in these structures [27]. The recent discovery of the promising properties and applications of two-dimensional glide-symmetric structures has encouraged the development of new fast and efficient methods to model and describe their characteristics.

The homogenized impedance model has been widely used to model different types of periodic structures [28], [29]. Unfortunately, this model is not applicable to glide-symmetric structures due to the fact that in this case there are two strongly coupled surfaces and higher-order modes are inevitably required [30]. Therefore, glide-symmetric structures cannot rigorously be modeled by the analysis of just one of the surfaces [31]. The use of formulations based on integral equations [32]–[37] would be very

flexible in terms of geometries and materials. However, a purely numerical approach would prevent from deriving a simple dispersion equation highlighting the difference between glide and non-glide surfaces. Thus, a mode matching technique [38] is here proposed. Previously, approaches of this kind have been devoted to efficiently analyze the dispersion characteristics of strongly interacting corrugated surfaces [39], [40] and holey surfaces with square holes [41], [42], including glide-symmetric ones [43]. These recent works have provided information on the behavior of the fields excited inside the holes and demonstrated that considering only the dominant mode inside the hole, as in non-glide holey structures [44], does not model the structure accurately [41], [42]. In addition, the presented results in these works have proved that the proposed mode-matching method is faster and more efficient than commercial software based on the finite-method algorithms such as *CST Microwave Studio*, especially when the hole is large or the gap between the two surfaces is very small.

In the mode matching formulation presented in [43], to analyze glide-symmetric holey structures with rectangular holes, the higher symmetry and the generalized Floquet theorem proposed in [27] were applied to reduce the computational domain to one half of the unit cell. As a result, the method not only becomes more efficient than previous mode-matching methods [40], but also it provides a physical insight into the specific properties of Floquet harmonics propagating in the structures caused by the higher symmetry. However, in practical applications, cylindrical or conical holes are easier to manufacture, since they only require of drilling, instead of milling. In this paper, we extend the mode-matching formulation presented in [43] to analyze glide-symmetric holey structures with an arbitrary shape of the hole. We demonstrate that the analysis of a glide-symmetric holey unit cell with the distance g between the layers (Fig. 1(a)), has the same complexity of its corresponding non-glide unit cell consisting of one layer holey surface with a perfectly electric conductor (PEC) plane at the distance of $g/2$ above it (Fig. 1(b)). Note that the non-glide structure is considered here with a gap of $g/2$ since we show later that the analysis of the two unit cells can be carried out similarly.

Our formulation is validated for the specific case of cylindrical holes by comparing our mode matching with the results obtained from the commercial software *CST Microwave Studio* for different values of the unit cell parameters. The results confirm the possibility of tuning the effective refractive index by adjusting the geometric parameters, as well as, the lack of the frequency dispersion for the first propagating mode due to the absence of the stop-band between the first and second modes. Thus, our method can be applied to design the unit cell of all-metal glide-symmetric holey metasurfaces that can be used in low-cost and low-loss graded-index planar lenses and gap waveguide technology.

The paper is organized as below. In Section II, the general mode matching formulation to analyze glide-symmetric all-metal holey structures is presented. In Section III, numerical implementations for the case with cylindrical holes is explained. In Section IV, numerical results for the case with cylindrical holes with different physical parameters are used to validate our method and demonstrate the possibility of tuning effective refractive index. Section V summarizes the conclusions of our work.

II. FORMULATION

In this section, the structures illustrated in Fig. 1 are analyzed in parallel using a mode matching technique. Both structures are bounded along the z-direction and periodic along the x- and y-direction with a periodicity of d. In addition, in both, the holes and the gap between the layers are filled with air. However, one of them is a glide-symmetric holey metasurface which has a gap of g between two layers (Fig. 1(a)) and the other one is a conventional holey metasurface with a PEC plane above it at the distance of $g/2$ (Fig. 1(b)). Note that the plane $z = 0$ is located in the middle of the gap for the former and on the PEC plane for the latter. We will demonstrate that employing a generalized Floquet theorem, the dispersion equation for these two structures is the same except a function related to the vertical wave number of the Floquet modes.

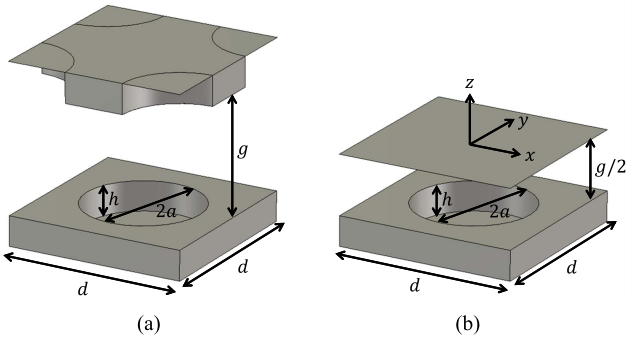

FIGURE 1. Unit cell of (a) a glide-symmetric holey structure, (b) a periodic holey structure with a PEC plane above it.

For both structures, the tangential fields inside the waveguide can be expressed as

$$\mathbf{E}_t^{WG}(\boldsymbol{\rho}, z = -g/2) = \sum_{m=1}^{M} r_m^- C_m \boldsymbol{\Phi}_m(\boldsymbol{\rho}) \tag{1}$$

$$\mathbf{H}_t^{WG}(\boldsymbol{\rho}, z = -g/2) = \sum_{m=1}^{M} r_m^+ Y_m C_m \left[\hat{z} \times \boldsymbol{\Phi}_m(\boldsymbol{\rho})\right] \tag{2}$$

where C_m is the unknown coefficient of the m-th mode and $\boldsymbol{\Phi}_m$ and Y_m are the corresponding cross section modal function and wave admittance of the m-th mode. Note that, for brevity, we do not distinguish between TE and TM modes which means the value of m indicates if the mode is TE or TM. Additionally,

$$r_m^{\pm} = 1 \pm \exp\left(-j2k_{zm}h\right) \tag{3}$$

are the magnetic-field and electric-field reflection coefficients due to the short circuit at the end of the waveguide, where $k_{zm} = \sqrt{k_0^2 - k_{tm}^2}$ is the longitudinal wavenumber and k_{tm} is the transversal wavenumber.

Additionally, for both structures, the fields in the gap region can be expressed based on Floquet harmonics:

$$E_t^{\text{Gap}} = \frac{1}{d^2} \sum_{pq} e^{-j(k_{x,p}x + k_{y,q}y)} \tilde{\mathbf{e}}_{t,pq}^{\text{Gap}}(z) \tag{4}$$

$$H_t^{\text{Gap}} = \frac{1}{d^2} \sum_{pq} e^{-j(k_{x,p}x + k_{y,q}y)} \tilde{\mathbf{h}}_{t,pq}^{\text{Gap}}(z) \tag{5}$$

where $k_{x,p} = k_{x,0} + 2\pi p/d$, $k_{y,q} = k_{y,0} + 2\pi p/d$, and p and q are the integer values identifying the order of the Floquet harmonics. The amplitude of each Floquet harmonic of the transversal electric and magnetic fields can be written as:

$$\tilde{\mathbf{e}}_{t,pq}^{\text{Gap}}(z) = \begin{pmatrix} A_{pq}^x \\ A_{pq}^y \end{pmatrix} \sin(k_{z,pq}z) + \begin{pmatrix} B_{pq}^x \\ B_{pq}^y \end{pmatrix} \cos(k_{z,pq}z) \tag{6}$$

$$\tilde{\mathbf{h}}_{t,pq}^{\text{Gap}}(z) = \begin{pmatrix} D_{pq}^x \\ D_{pq}^y \end{pmatrix} \sin(k_{z,pq}z) + \begin{pmatrix} F_{pq}^x \\ F_{pq}^y \end{pmatrix} \cos(k_{z,pq}z), \tag{7}$$

where $k_{z,pq} = \sqrt{k_0^2 - k_{x,p}^2 - k_{y,q}^2}$ is the vertical wave number of the (p, q)th harmonic. From Maxwell equations, we can derive the relation between the A and B coefficients in (6) and the D and F coefficients in (7) [43].

Imposing the continuity of the tangential electric field at the lower surface $z = -g/2$, we have, for both structures,

$$\mathbf{E}_t^{\text{Gap}}(x, y, z = -g/2) = \mathbf{E}_t^{\text{WG}}(x, y, z = -g/2). \tag{8}$$

Substituting the modal expansion (1) and Floquet expansion (4) into (8),

$$\frac{1}{d^2} \sum_{pq} e^{-j(k_{x,p}x + k_{y,q}y)} \tilde{\mathbf{e}}_{t,pq}^{\text{Gap}}(z = -g/2) = \sum_{m=1}^{M} r_m^- C_m \boldsymbol{\Phi}_m(\boldsymbol{\rho}), \tag{9}$$

and inverting, we obtain

$$\tilde{\mathbf{e}}_{t,pq}^{\text{Gap}}(z = -g/2) = \sum_m r_m^- C_m \tilde{\boldsymbol{\Phi}}_m(k_{x,p}, k_{y,q}). \tag{10}$$

The right hand side of the above equation is the Fourier transforms of $\mathbf{E}_t^{\text{WG}}(\boldsymbol{\rho}, z = -g/2)$ expressed in (1) and denoted by $\tilde{\mathbf{E}}_t^{\text{WG}}\left(k_{x,p}, k_{y,q}\right)$. Thus,

$$\tilde{\mathbf{e}}_{t,pq}^{\text{Gap}}(z = -g/2) = \tilde{\mathbf{E}}_t^{\text{WG}}\left(k_{x,p}, k_{y,q}\right). \tag{11}$$

Consequently, $\tilde{\boldsymbol{\Phi}}_m\left(k_{x,p}, k_{y,q}\right)$ are the Fourier transforms of the modal functions $\boldsymbol{\Phi}_m$:

$$\begin{aligned} \tilde{\boldsymbol{\Phi}}_m(k_{x,p}, k_{y,q}) &= \hat{x}\tilde{\phi}_m^x(k_{x,p}, k_{y,q}) + \hat{y}\tilde{\phi}_m^y(k_{x,p}, k_{y,q}) \\ &= \int_{S_{hole}} \boldsymbol{\Phi}_m(\boldsymbol{\rho}) e^{j(k_{x,p}x + k_{y,q}y)} ds \end{aligned} \tag{12}$$

For the non-glide structure, the continuity of the electric field on the upper surface ($z = 0$) yields

$$\mathbf{E}_t^{\text{Gap}}(x, y, z = 0) = \mathbf{0}. \tag{13}$$

However, for the glide-symmetric case, the continuity of the electric field on the upper surface ($z = g/2$) can be written as

$$\begin{aligned} &\mathbf{E}_t^{\text{Gap}}(x, y, z = g/2) \\ &\quad = e^{-j(k_{x,0}d + k_{y,0}d)/2} \mathbf{E}_t^{\text{WG}}(x - \frac{d}{2}, y - \frac{d}{2}, z = -\frac{g}{2}), \end{aligned} \tag{14}$$

using the generalized Floquet theorem [43]. If the Floquet series (4) is replaced into (13) and (14) and inverted by means of the Fourier-transform properties, we obtain, respectively,

$$\tilde{\mathbf{e}}_{t,pq}^{\text{Gap}}(z = 0) = \mathbf{0}, \tag{15}$$

$$\tilde{\mathbf{e}}_{t,pq}^{\text{Gap}}(z = g/2) = (-1)^{p+q} \tilde{\mathbf{E}}_t^{\text{WG}}\left(k_{x,p}, k_{y,q}\right). \tag{16}$$

Solving two vector equations (11) and (15) for the non-glide structure and (11) and (16) for the glide-symmetric case, the unknown coefficients A and B in (6) can be expressed as functions of the modal-waveguide coefficients C.

For the non-glide case, we have

$$\begin{aligned} \begin{pmatrix} A_{pq}^x \\ A_{pq}^y \end{pmatrix} &= -\frac{\tilde{\mathbf{E}}_t^{\text{WG}}\left(k_{x,p}, k_{y,q}\right)}{\sin\left(k_{z,pq}g/2\right)} \\ \begin{pmatrix} B_{pq}^x \\ B_{pq}^y \end{pmatrix} &= \mathbf{0}. \end{aligned} \tag{17}$$

However, for the glide-symmetric case, if $p + q$ is even,

$$\begin{aligned} \begin{pmatrix} A_{pq}^x \\ A_{pq}^y \end{pmatrix} &= \mathbf{0} \\ \begin{pmatrix} B_{pq}^x \\ B_{pq}^y \end{pmatrix} &= \frac{\tilde{\mathbf{E}}_t^{\text{WG}}\left(k_{x,p}, k_{y,q}\right)}{\cos\left(k_{z,pq}g/2\right)}, \end{aligned} \tag{18}$$

and if $p + q$ is odd,

$$\begin{aligned} \begin{pmatrix} A_{pq}^x \\ A_{pq}^y \end{pmatrix} &= -\frac{\tilde{\mathbf{E}}_t^{\text{WG}}\left(k_{x,p}, k_{y,q}\right)}{\sin\left(k_{z,pq}g/2\right)} \\ \begin{pmatrix} B_{pq}^x \\ B_{pq}^y \end{pmatrix} &= \mathbf{0}. \end{aligned} \tag{19}$$

Considering these results, an interesting symmetry property of Floquet harmonics can be seen in glide-symmetric structures, i.e. if the parity of a (p, q) Floquet harmonic is defined as the parity of the number $p + q$, it is clear that even (odd) harmonics have an even (odd) transverse electric field along the z direction with respect to the glide plane ($z = 0$). The same conclusion has been demonstrated for the glide-symmetric corrugation and glide-symmetric holey structure with square holes in [43]. Indeed, as shown in (18) and (19), this conclusion is valid for all glide-symmetric holey structures regardless of the shape of the hole.

Now that the A and B coefficients are expressed in terms of the C coefficients, using Maxwell equations, D and F coefficients in (7) can be also expressed in terms of the

C coefficients. Substituting these expressions into (7), for $\tilde{\mathbf{h}}^{\text{Gap}}_{t,pq}(z=-g/2)$ we obtain:

$$\begin{aligned} &jk_0\eta_0\tilde{h}^{\text{Gap}}_{x,pq}(z=-g/2) \\ &\quad= +\frac{k_{x,p}k_{y,q}}{k_{z,pq}}\tilde{f}_{pq}(k_{z,pq})\sum_m r_m^- C_m\tilde{\phi}^x_m(k_{x,p},k_{y,q}) \\ &\qquad+\frac{k_0^2-k_{x,p}^2}{k_{z,pq}}\tilde{f}_{pq}(k_{z,pq})\sum_m r_m^- C_m\tilde{\phi}^y_m(k_{x,p},k_{y,q}) \end{aligned} \tag{20a}$$

$$\begin{aligned} &jk_0\eta_0\tilde{h}^{\text{Gap}}_{y,pq}(z=-g/2) \\ &\quad= -\frac{k_{x,p}k_{y,q}}{k_{z,pq}}\tilde{f}_{pq}(k_{z,pq})\sum_m r_m^- C_m\tilde{\phi}^y_m(k_{x,p},k_{y,q}) \\ &\qquad-\frac{k_0^2-k_{y,q}^2}{k_{z,pq}}\tilde{f}_{pq}(k_{z,pq})\sum_m r_m^- C_m\tilde{\phi}^x_m(k_{x,p},k_{y,q}) \end{aligned} \tag{20b}$$

where $\tilde{f}_{pq}(k_{z,pq})$ is called the vertical spectral function and defined as

$$\tilde{f}_{pq}(k_{z,pq}) = \cot(k_{z,pq}g/2) \tag{21}$$

for the non-glide structure and

$$\tilde{f}_{pq} = \begin{cases} -\tan\left(k_{z,pq}g/2\right) & p+q \quad \text{even} \\ \cot\left(k_{z,pq}g/2\right) & p+q \quad \text{odd} \end{cases} \tag{22}$$

for the glide structure.

Now, by enforcing the continuity of the tangential magnetic fields (2) and (5) across the hole aperture at $z=-g/2$, the dispersion equation can be derived. Note that it is not needed to enforce the continuity of the tangential magnetic field on the upper surface $z=g/2$ in the glide structure as the generalized Floquet theorem confirms its satisfaction because of the symmetry of the structure. Thus, to obtain the dispersion equation, first, we set (2) and (5) equal:

$$\begin{aligned} &\sum_{m=1}^{M} r_m^+ Y_m C_m\left[\hat{z}\times\boldsymbol{\Phi}_m(\boldsymbol{\rho})\right] \\ &\qquad= \frac{1}{d^2}\sum_{pq} e^{-j(k_{x,p}x+k_{y,q}y)}\tilde{\mathbf{h}}^{\text{Gap}}_{t,pq}(z=-g/2). \end{aligned} \tag{23}$$

Then, by the cross product of each waveguide modal function $\boldsymbol{\Phi}_n(\boldsymbol{\rho})$ and the above boundary condition equation, and integrating over the hole surface, we obtain

$$\begin{aligned} &\hat{z}\sum_{m=1}^{M} r_m^+ Y_m C_m I_{nm} \\ &\qquad= \frac{1}{d^2}\sum_{pq}\tilde{\boldsymbol{\Phi}}_n\left(-k_{x,p},-k_{y,q}\right)\times\tilde{\mathbf{h}}^{\text{Gap}}_{t,pq}(z=-g/2), \end{aligned} \tag{24}$$

where

$$I_{nm} = \int_{S_{hole}} \boldsymbol{\Phi}_n(\boldsymbol{\rho})\cdot\boldsymbol{\Phi}_m(\boldsymbol{\rho})ds. \tag{25}$$

Assuming that the structure is made of perfectly conducting metals, the modal functions are orthogonal over S_{hole}, regardless of the shape of the cross section [45]. Thus, $I_{nm}=0$ when $m\neq n$. Substituting (20) in (24) and rearranging the equation, we obtain a set of linear equations:

$$\sum_{m=1}^{M}\alpha_{n,m}C_m = 0 \quad n=1,\ldots,M \tag{26}$$

where M is the number of modal functions,

$$\alpha_{n,m} = jk_0\eta_0\, d^2 Y_m I_{nm} + \frac{r_m^-}{r_m^+}\sum_{pq}\tilde{f}_{pq}(k_{z,pq})\beta_{n,m}(\mathbf{k}_{pq}) \tag{27}$$

and

$$\begin{aligned} \beta_{n,m}(\mathbf{k}_{pq}) &= \beta_{n,m}(k_{x,p},k_{y,q},k_{z,pq}) \\ &= \frac{k_0^2-k_{y,q}^2}{k_{z,pq}}\tilde{\phi}^x_m(k_{x,p},k_{y,q})\tilde{\phi}^x_n(-k_{x,p},-k_{y,q}) \\ &\quad+\frac{k_{x,p}k_{y,q}}{k_{z,pq}}\tilde{\phi}^y_m(k_{x,p},k_{y,q})\tilde{\phi}^x_n(-k_{x,p},-k_{y,q}) \\ &\quad+\frac{k_0^2-k_{x,p}^2}{k_{z,pq}}\tilde{\phi}^y_m(k_{x,p},k_{y,q})\tilde{\phi}^y_n(-k_{x,p},-k_{y,q}) \\ &\quad+\frac{k_{x,p}k_{y,q}}{k_{z,pq}}\tilde{\phi}^x_m(k_{x,p},k_{y,q})\tilde{\phi}^y_n(-k_{x,p},-k_{y,q}). \end{aligned} \tag{28}$$

Setting the determinant of the coefficient matrix in (26) equal to zero, the dispersion equation follows. The roots of this equation can be found by either applying a zero-finding algorithm [46] or simply searching for the minimum of the magnitude of the determinant.

Note that the presented formulation is valid for all holey periodic structures regardless of the shape of the hole, if the structure possesses glide symmetry or not, and whether the holey structure is bounded (by a metallic plane above) or unbounded. For different shapes of the holes, the appropriate modal functions $\boldsymbol{\Phi}_m$ must be found and substituted in the formulation. The difference between the non-glide and glide cases are distinguished with the correct definition of $\tilde{f}_{pq}(k_{z,pq})$ (see (21) and (22)). Finally, in the case of unbounded structure (a holey periodic structure in the air), we have $g\to+\infty$ and all $k_{z,pq}$ are imaginary for bound (non-radiating) modes. Thus, in (21), $\tilde{f}_{pq}(k_{z,pq})\to j$, which means it is enough to replace $\tilde{f}_{pq}(k_{z,pq})$ with j in the formulation. In summary, the vertical spectral function $\tilde{f}_{pq}(k_{z,pq})$ specifies if the holey periodic structure is unbounded, bounded with a PEC plane above it, or bounded in a glide-symmetric configuration.

III. NUMERICAL IMPLEMENTATION FOR CYLINDRICAL HOLES

For holes with circular cross section, $\boldsymbol{\Phi}_m(\boldsymbol{\rho}) = \hat{\rho}E_{\rho m}+\hat{\varphi}E_{\varphi m}$. For numerical implementation, we need to make a look up table by arranging the propagating modes inside the holes based on their cut-off frequencies. In case of a cylindrical waveguide, the modes are sorted as TE_{11}, TM_{01}, TE_{21}, TE_{01}, TM_{11}, etc. For all TE and TM modes, except those that have azimuthal symmetry such as TM_{01} or TE_{01}, the variation with respect to φ specifies two degenerate modes. However,

we assume two terms in the series in (1) for all the modes including those with azimuthal symmetry. This means we assume $M = 2N$ in (1), where N is the number of considered modes inside the holes, where $n = 1$ corresponds to the first dominant mode (TE_{11}), $n = 2$ corresponds to the second one (TM_{01}), and so on. Note that considering two terms in the modal expansion for the azimuthal symmetric modes produces all zero rows and columns in the final coefficient matrix. These rows and columns must be excluded before calculating the determinant of the matrix. Thus, for each mode (each n), there are two terms in the series in (1), $m = 2n - 1$ and $m = 2n$. We allocate odd values of m for the modes whose φ-dependency of their $E_{\rho m}$ is expressed with a sine function and even values of m for the modes whose φ-dependency of their $E_{\rho m}$ is expressed with a cosine function. Thus, if n corresponds to a TE mode (let us say TE_{rs}), $Y_m = k_{zm}/(\eta_0 k_0)$ for $m = 2n - 1$ and $m = 2n$, and we have [45]

$$\begin{cases} E_{\rho m} = +\dfrac{r}{\rho} J_r\left(\dfrac{x'_{r,s}}{a}\rho\right)\sin(r\varphi) \\ E_{\varphi m} = \dfrac{x'_{r,s}}{a} J'_r\left(\dfrac{x'_{r,s}}{a}\rho\right)\cos(r\varphi) \end{cases} \quad if \quad m = 2n-1, \tag{29}$$

$$\begin{cases} E_{\rho m} = -\dfrac{r}{\rho} J_r\left(\dfrac{x'_{r,s}}{a}\rho\right)\cos(r\varphi) \\ E_{\varphi m} = \dfrac{x'_{r,s}}{a} J'_r\left(\dfrac{x'_{r,s}}{a}\rho\right)\sin(r\varphi) \end{cases} \quad if \quad m = 2n. \tag{30}$$

Similarly, if n corresponds to a TM mode (let us say TM_{rs}), $Y_m = k_0/(\eta_0 k_{zm})$ for $m = 2n - 1$ and $m = 2n$, and we have [45]

$$\begin{cases} E_{\rho m} = \dfrac{x_{r,s}}{a} J'_r\left(\dfrac{x_{r,s}}{a}\rho\right)\sin(r\varphi) \\ E_{\varphi m} = +\dfrac{r}{\rho} J_r\left(\dfrac{x_{r,s}}{a}\rho\right)\cos(r\varphi) \end{cases} \quad if \quad m = 2n-1, \tag{31}$$

$$\begin{cases} E_{\rho m} = \dfrac{x_{r,s}}{a} J'_r\left(\dfrac{x_{r,s}}{a}\rho\right)\cos(r\varphi) \\ E_{\varphi m} = -\dfrac{r}{\rho} J_r\left(\dfrac{x_{r,s}}{a}\rho\right)\sin(r\varphi) \end{cases} \quad if \quad m = 2n. \tag{32}$$

Note that in the above field expressions, a is the radius of the circular holes, J_r and J'_r are the Bessel function of the first kind and its first derivative, and $x_{r,s}$ and $x'_{r,s}$ are the s-th root of J_r and J'_r.

After expressing the modal functions $\mathbf{\Phi}_m(\boldsymbol{\rho})$, the integrals in (12) and (25) must be calculated to obtain $\tilde{\mathbf{\Phi}}_m(k_{x,p}, k_{y,q})$ and I_{mm}. In this case, the results of these integrals can be expressed in closed form. However, for an arbitrary cross section, numerical integration methods might be used to calculate the integrals. Finally, note once $\tilde{\mathbf{\Phi}}_m(k_{x,p}, k_{y,q})$ is calculated, $\tilde{\mathbf{\Phi}}_m(-k_{x,p}, -k_{y,q})$ is readily known since they are complex conjugate of each other.

IV. RESULTS

As mentioned in Section I, all-metal glide-symmetric mesurfaces tailored with cylindrical holes are a good candidate for designing low-loss graded-index planar lenses. In these lenses, by changing the radius or the depth of the holes, a spatial variation of the refractive index is achieved.

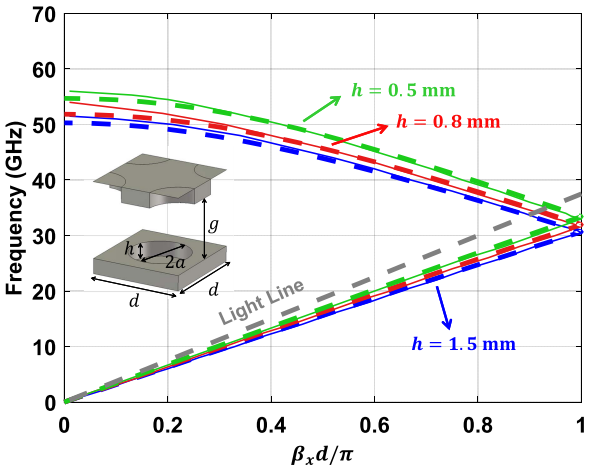

FIGURE 2. Dispersion diagram of the glide-symmetric unit cell with cylindrical holes as described in Fig. 1(a) with parameters: $d = 4$ mm, $a = 1.6$ mm, and $g = 0.2$ mm. The results were obtained for three values of h. Our proposed mode matching technique is represented with solid lines and *CST* simulations with dashed lines.

In this section, these structures are analyzed through their dispersion diagrams using the mode matching formulation presented in Section II. In addition, the possibility of tuning the effective refractive index is demonstrated. The code is implemented in Matlab and the results are compared with the ones obtained from commercial software *CST Microwave Studio*.

Our reference case has a gap between the surfaces with $g = 0.2$ mm, its period is $d = 4$ mm, a hole depth of $h = 1.5$ mm, and a hole radius of $a = 1.6$ mm. The influence of the relevant geometrical parameters on the equivalent refractive index is here investigated. Note that, for a fair comparison of the results, the same periodicity is assumed in all cases.

Fig. 2 shows the dispersion diagram of the reference case and its comparison with two cases with different depth of holes: $h = 0.5$ mm and $h = 0.8$ mm. The mode matching results are in good agreement with those of *CST*. The results also demonstrate that by increasing the depth of the holes, the equivalent refractive index increases too. However, it should be noted that, depending on the size of the hole and the frequency, after a certain depth, the equivalent refractive index does not increase any more by increasing h. The reason is that the hole size is subwavelength which causes the modes inside the holes attenuating exponentially when they travel toward the bottom of the hole. Increasing the hole depth beyond a certain value does not change significantly the field distribution in the overall structure.

In Fig. 3, the effect of variation of the hole radius is investigated. Again, the reference case is analyzed along with two cases with different values of hole radius: $a = 1.3$ mm and $a = 1$ mm. For all cases, the mode matching results are compared with *CST* simulations and a good agreement

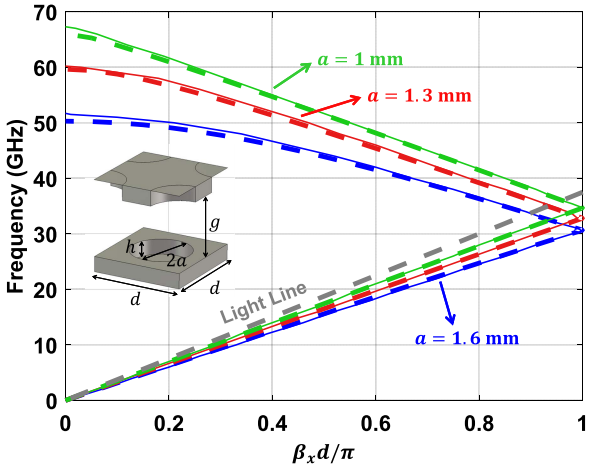

FIGURE 3. Dispersion diagram of the glide-symmetric unit cell with cylindrical holes as described in Fig. 1(a) with parameters: $d = 4$ mm, $h = 1.5$ mm, and $g = 0.2$ mm. The results were obtained for three values of a. Our proposed mode matching technique is represented with solid lines and *CST* simulations with dashed lines.

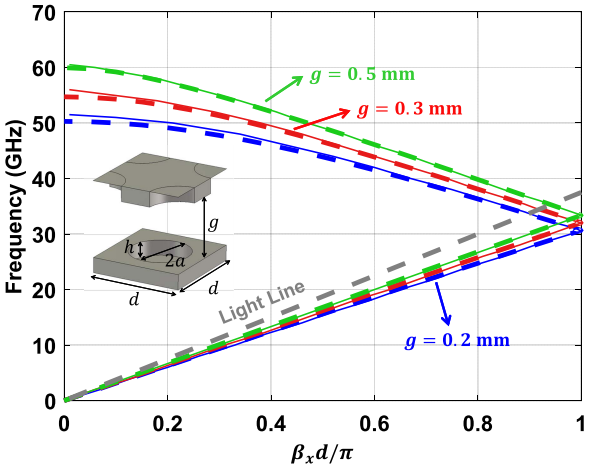

FIGURE 4. Dispersion diagram of the glide-symmetric unit cell with cylindrical holes as described in Fig. 1(a) with parameters: $d = 4$ mm, $a = 1.6$ mm, and $h = 1.5$ mm. The results were obtained for three values of g. Our proposed mode matching technique is represented with solid lines and *CST* simulations with dashed lines.

is achieved. By decreasing the radius, the propagation tends to approach the free-space limit, which means the equivalent refractive index becomes smaller. Smaller holes have a lower effect in the propagation inside the paralell plate.

Although in common practical applications the gap thickness is fixed and does not change to obtain a spatial variation of the refractive index, the influence of its variation on the dispersion diagram is here investigated. The comparison between the dispersion diagrams of the reference case and two values of gap, $g = 0.3$ mm and $g = 0.5$ mm, are depicted in Fig. 4. As in the two previous cases, a good agreement between the mode matching and *CST* results is achieved. By decreasing the thickness of the gap, the interaction between the surfaces becomes stronger, which causes a higher equivalent refractive index.

To show the full potential of our method, the dispersion diagram of the reference glide-symmetric structure and its

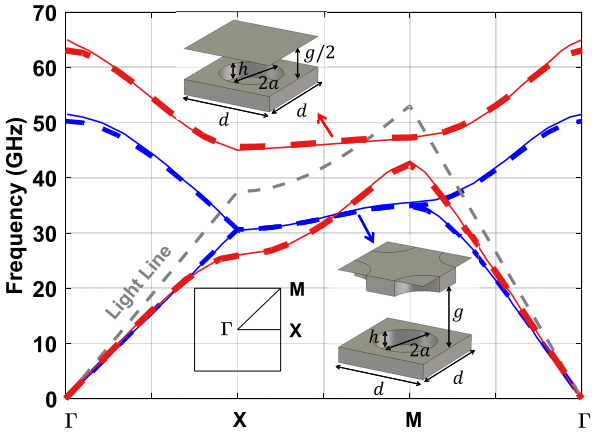

FIGURE 5. Dispersion diagram of the structures shown in Fig. 1(a) and 1(b) with parameters: $d = 4$ mm, $g = 0.2$ mm, $a = 1.6$ mm, and $h = 1.5$ mm, obtained with the proposed mode matching technique (solid lines) and *CST* simulation (dashed lines).

corresponding non-glide structure over the irreducible Brillouin zone is depicted in Fig. 5 and compared with *CST* simulation results. This type of simulation is typically carried out for designing EBG structures, which find application, for example, in gap waveguide technology.

In order to give an estimation of the speed of our method, we launched the simulations of CST and our code in the same computer. The computer had an Intel(R) Core(TM) i7-4790 CPU @3.6 GHz with 32 GB of RAM. All the presented results were obtained by considering the first eight dominant modes inside the cylindrical waveguide and setting $p = -2, ..., 2$ and $q = -2, ..., 2$ in (4) and (5). Additionally, the zeros of the determinant of the coefficient matrix in (26) were found by searching for the minimum of the magnitude of the determinant. With these choices, less than 0.5 s are required to obtain the β_x for a single frequency point with our mode-matching code. However, it takes 20 s to obtain the same result with *CST*. Only for the non-glide cases with 0.1 mm gap between the layers, the first eleven dominant modes inside the circular waveguide and $p, q = -3, ..., 3$ are selected, which increased the mode matching time to 0.8 s. The proposed method could become even faster by employing a zero-finding algorithm [46] to locate the zeros of the determinant in (26), instead of searching for the minimum of the magnitude of the determinant.

Finally, it is worth to comment on the number of modes we took into account in the waveguide region and the gap region. It is well-known that in mode-matching techniques, the convergence can be achieved if the modes in different regions match properly with each others. It usually requires to maintain an optimal ratio between the number of modes in different regions. For the presented cases, we found that the optimal ratio between the number of waveguide modes to Floquet modes is approximately 1.5.

V. DISCUSSION AND CONCLUSION

Here, we have proposed a general mode-matching formulation for developing dispersion analyses of holey surfaces in

the vicinity of a metal plane and a glide-symmetric holey surface. Our method can be applied to an arbitrary shape of the holes. As in our previous work presented in [43], for the case with glide symmetry, the higher symmetry of the structure and the generalized Floquet theorem are applied to reduce the computational cost.

The formulation was tested and verified for cases with cylindrical holes, which is of interest, in practice, for designing of low-cost and low-loss graded-index planar lenses and EBG structures. The code was checked for different values of geometrical parameters and for propagation in different directions, obtaining the irreducible Brillouin zone. For all cases, the mode-matching results show an excellent agreement with *CST* results. However, small variations are found at very high frequencies where the group velocity is near to zero. These small discrepancies do not have a significant effect on the obtained effective refractive indexes that would be used to design lenses.

Our proposed method is faster than the *CST* eigenmode solver since *CST* needs to mesh the whole volume of the unit cell, while in the mode matching formulation only the mode coefficients in one hole of the unit cell are calculated. We demonstrated that the second glide-symmetric hole does not add additional unknowns thanks to the enforced symmetry condition. Finally, the proposed method can be extended to account for losses and characterize complex wavenumbers. However, this is not possible with *CST* eigenmode solver.

REFERENCES

[1] H.-T. Chen, A. J. Taylor, and N. Yu, "A review of metasurfaces: Physics and applications," *Rep. Prog. Phys.*, vol. 79, no. 7, p. 076401, 2016. [Online]. Available: http://stacks.iop.org/0034-4885/79/i=7/a=076401

[2] S. Maci, G. Minatti, M. Casaletti, and M. Bosiljevac, "Metasurfing: Addressing waves on impenetrable metasurfaces," *IEEE Antennas Wireless Propag. Lett.*, vol. 10, pp. 1499–1502, 2011.

[3] C. Pfeiffer and A. Grbic, "A printed, broadband luneburg lens antenna," *IEEE Trans. Antennas Propag.*, vol. 58, no. 9, pp. 3055–3059, Sep. 2010.

[4] M. Bosiljevac, M. Casaletti, F. Caminita, Z. Sipus, and S. Maci, "Non-uniform metasurface luneburg lens antenna design," *IEEE Trans. Antennas Propag.*, vol. 60, no. 9, pp. 4065–4073, Sep. 2012.

[5] P.-S. Kildal, E. Alfonso, A. Valero-Nogueira, and E. Rajo-Iglesias, "Local metamaterial-based waveguides in gaps between parallel metal plates," *IEEE Antennas Wireless Propag. Lett.*, vol. 8, no. 4, pp. 84–87, Apr. 2009.

[6] P.-S. Kildal, A. U. Zaman, E. Rajo-Iglesias, E. Alfonso, and A. Valero-Nogueira, "Design and experimental verification of ridge gap waveguide in bed of nails for parallel-plate mode suppression," *IET Microw., Antennas Propag.*, vol. 5, no. 3, pp. 262–270, Mar. 2011.

[7] R. Quesada, D. Martín-Cano, F. J. García-Vidal, and J. Bravo-Abad, "Deep-subwavelength negative-index waveguiding enabled by coupled conformal surface plasmons," *Opt. Lett.*, vol. 39, no. 10, pp. 2990–2993, May 2014. [Online]. Available: http://ol.osa.org/abstract.cfm?URI=ol-39-10-2990

[8] M. Camacho, R.-C. Mitchell-Thomas, A.-P. Hibbins, J.-R. Sambles, and O. Quevedo-Teruel, "Designer surface plasmon dispersion on a one-dimensional periodic slot metasurface with glide symmetry," *Opt. Lett.*, vol. 42, no. 17, pp. 3375–3378, 2017. [Online]. Available: http://ol.osa.org/abstract.cfm?URI=ol-42-17-3375

[9] M. Camacho, R. C. Mitchell-Thomas, A. P. Hibbins, J. R. Sambles, and O. Quevedo-Teruel, "Mimicking glide symmetry dispersion with coupled slot metasurfaces," *Appl. Phys. Lett.*, vol. 111, no. 2, p. 121603, 2017.

[10] P. Padilla, L. F. Herrán, A. Tamayo-Domínguez, J. F. Valenzuela-Valdés, and O. Quevedo-Teruel, "Glide symmetry to prevent the lowest stopband of printed corrugated transmission lines," *IEEE Microw. Wireless Compon. Lett.*, vol. 28, no. 9, pp. 750–752, Sep. 2018.

[11] O. Dahlberg, R. C. Mitchell-Thomas, and O. Quevedo-Teruel, "Reducing the dispersion of periodic structures with twist and polar glide symmetries," *Sci. Rep.*, vol. 7, Aug. 2017, Art. no. 10136.

[12] O. Quevedo-Teruel, O. Dahlberg, and G. Valerio, "Propagation in waveguides with transversal twist-symmetric holey metallic plates," *IEEE Microw. Wireless Compon. Lett.*, vol. 28, no. 10, pp. 858–860, Oct. 2018.

[13] F. Ghasemifard, M. Norgren, and O. Quevedo-Teruel, "Twist and polar glide symmetries: An additional degree of freedom to control the propagation characteristics of periodic structures," *Sci. Rep.*, vol. 8, Jul. 2018, Art. no. 11266.

[14] Q. Chen, F. Ghasemifard, G. Valerio, and O. Quevedo-Teruel, "Modeling and dispersion analysis of coaxial lines with higher symmetries," *IEEE Trans. Microw. Theory Techn.*, vol. 66, no. 10, pp. 4338–4345, Oct. 2018.

[15] O. Quevedo-Teruel, M. Ebrahimpouri, and M. N. M. Kehn, "Ultrawideband metasurface lenses based on off-shifted opposite layers," *IEEE Antennas Wireless Propag. Lett.*, vol. 15, pp. 484–487, 2016.

[16] R. C. Mitchell-Thomas, J. R. Sambles, and A. P. Hibbins, "High index metasurfaces for graded lenses using glide symmetry," in *Proc. 11th Eur. Conf. Antennas Propag. (EUCAP)*, Mar. 2017, pp. 1396–1397.

[17] K. Liu, F. Ghasemifard, and O. Quevedo-Teruel, "Broadband metasurface luneburg lens antenna based on glide-symmetric bed of nails," in *Proc. 11th Eur. Conf. Antennas Propag. (EuCAP)*, Mar. 2017, pp. 358–360.

[18] O. Quevedo-Teruel, M. Ebrahimpouri, and F. Ghasemifard, "Lens antennas for 5G communications systems," *IEEE Commun. Mag.*, vol. 56, no. 7, pp. 36–41, Jul. 2018.

[19] O. Quevedo-Teruel, J. Miao, M. Mattsson, A. Algaba-Brazalez, M. Johansson, and L. Manholm, "Glide-symmetric fully metallic luneburg lens for 5G communications at Ka-band," *IEEE Antennas Wireless Propag. Lett.*, vol. 17, no. 9, pp. 1588–1592, Sep. 2018.

[20] M. Ebrahimpouri, O. Quevedo-Teruel, and E. Rajo-Iglesias, "Design guidelines for gap waveguide technology based on glide-symmetric holey structures," *IEEE Microw. Wireless Compon. Lett.*, vol. 27, no. 6, pp. 542–544, Jun. 2017.

[21] M. Ebrahimpouri, E. Rajo-Iglesias, Z. Sipus, and O. Quevedo-Teruel, "Cost-effective gap waveguide technology based on glide-symmetric holey EBG structures," *IEEE Trans. Microw. Theory Techn.*, vol. 66, no. 2, pp. 927–934, Feb. 2018.

[22] M. Ebrahimpouri, A. A. Brazalez, L. Manholm, and O. Quevedo-Teruel, "Using glide-symmetric holes to reduce leakage between waveguide flanges," *IEEE Microw. Wireless Compon. Lett.*, vol. 28, no. 6, pp. 473–475, Jun. 2018.

[23] E. Rajo-Iglesias, M. Ebrahimpouri, and O. Quevedo-Teruel, "Wideband phase shifter in groove gap waveguide technology implemented with glide-symmetric holey EBG," *IEEE Microw. Wireless Compon. Lett.*, vol. 28, no. 6, pp. 476–478, Jun. 2018.

[24] P. J. Crepeau and P. R. McIsaac, "Consequences of symmetry in periodic structures," *Proc. IEEE*, vol. 52, no. 1, pp. 33–43, Jan. 1964.

[25] R. Mittra and S. Laxpati, "Propagation in a wave guide with glide reflection symmetry," *Can. J. Phys.*, vol. 43, pp. 353–372, Feb. 1965.

[26] R. B. Kieburtz and J. Impagliazzo, "Multimode propagation on radiating traveling-wave structures with glide-symmetric excitation," *IEEE Trans. Antennas Propag.*, vol. AP-18, no. 1, pp. 3–7, Jan. 1970.

[27] A. Hessel, M. H. Chen, R. C. M. Li, and A. A. Oliner, "Propagation in periodically loaded waveguides with higher symmetries," *Proc. IEEE*, vol. 61, no. 2, pp. 183–195, Feb. 1973.

[28] Z. Sipus, H. Merkel, and P.-S. Kildal, "Green's functions for planar soft and hard surfaces derived by asymptotic boundary conditions," *IEE Proc. Microw., Antennas Propag.*, vol. 144, no. 5, pp. 321–328, Oct. 1997.

[29] M. Bosiljevac, Z. Sipus, and P. S. Kildal, "Construction of Green's functions of parallel plates with periodic texture with application to gap waveguides—A plane-wave spectral-domain approach," *IET Microw., Antennas Propag.*, vol. 4, no. 11, pp. 1799–1810, Nov. 2010.

[30] G. Valerio, Z. Sipus, A. Grbic, and O. Quevedo-Teruel, "Accurate equivalent-circuit descriptions of thin glide-symmetric corrugated metasurfaces," *IEEE Trans. Antennas Propag.*, vol. 65, no. 5, pp. 2695–2700, May 2017.

[31] F. Mesa, R. Rodríguez-Berral, and F. Medina, "On the computation of the dispersion diagram of symmetric one-dimensionally periodic structures," *Symmetry*, vol. 10, no. 8, p. 307, 2018. [Online]. Available: http://www.mdpi.com/2073-8994/10/8/307

[32] A. F. Peterson, S. L. Ray, and R. Mittra, *Computational Methods for Electromagnetics*. Hoboken, NJ, USA: Wiley, 1997.

[33] G. Valerio, D. R. Wilton, D. R. Jackson, and A. Galli, "Acceleration of mixed potentials from vertical currents in layered media for 2-D structures with 1-D periodicity," *IEEE Trans. Antennas Propag.*, vol. 60, no. 8, pp. 3782–3793, Aug. 2012.
[34] R. Florencio, R. R. Boix, and J. A. Encinar, "Fast and accurate MoM analysis of periodic arrays of multilayered stacked rectangular patches with application to the design of reflectarray antennas," *IEEE Trans. Antennas Propag.*, vol. 63, no. 6, pp. 2558–2571, Jun. 2015.
[35] S. D. Gedney and R. Mittra, "Analysis of the electromagnetic scattering by thick gratings using a combined FEM/MM solution," *IEEE Trans. Antennas Propag.*, vol. 39, no. 11, pp. 1605–1614, Nov. 1991.
[36] A. Nicolet, S. Guenneau, C. Geuzaine, and F. Zolla, "Modelling of electromagnetic waves in periodic media with finite elements," *J. Comput. Appl. Math.*, vol. 168, nos. 1–2, pp. 321–329, 2004. [Online]. Available: http://www.sciencedirect.com/science/article/pii/S0377042703009956
[37] D. R. Wilton, T. F. Eibert, J. L. Volakis, and D. R. Jackson, "Hybrid FE/BI modeling of 3-D doubly periodic structures utilizing triangular prismatic elements and an MPIE formulation accelerated by the Ewald transformation," *IEEE Trans. Antennas Propag.*, vol. 47, no. 5, pp. 843–850, May 1999.
[38] A. Wexler, "Solution of waveguide discontinuities by modal analysis," *IEEE Trans. Microw. Theory Techn.*, vol. MTT-15, no. 9, pp. 508–517, Sep. 1967.
[39] F. Ghasemifard, M. Ebrahimpouri, M. Norgren, and O. Quevedo-Teruel, "Mode matching analysis of two dimensional glide-symmetric corrugated metasurfaces," in *Proc. 11th Eur. Conf. Antennas Propag. (EuCAP)*, Mar. 2017, pp. 749–751.
[40] F. Ghasemifard, M. Norgren, and O. Quevedo-Teruel, "Dispersion analysis of 2-D glide-symmetric corrugated metasurfaces using mode-matching technique," *IEEE Microw. Wireless Compon. Lett.*, vol. 28, no. 1, pp. 1–3, Jan. 2018.
[41] G. Valerio, Z. Sipus, A. Grbic, and O. Quevedo-Teruel, "Nonresonant modes in plasmonic holey metasurfaces for the design of artificial flat lenses," *Opt. Lett.*, vol. 42, no. 10, pp. 2026–2029, May 2017. [Online]. Available: http://ol.osa.org/abstract.cfm?URI=ol-42-10-2026
[42] F. J. G. de Abajo and J. J. Sáenz, "Electromagnetic surface modes in structured perfect-conductor surfaces," *Phys. Rev. Lett.*, vol. 95, p. 233901, Nov. 2005. [Online]. Available: https://link.aps.org/doi/10.1103/PhysRevLett.95.233901
[43] G. Valerio, F. Ghasemifard, Z. Sipus, and O. Quevedo-Teruel, "Glide-symmetric all-metal holey metasurfaces for low-dispersive artificial materials: Modeling and properties," *IEEE Trans. Microw. Theory Techn.*, vol. 66, no. 7, pp. 3210–3223, Jul. 2018.
[44] F. J. Garcia-Vidal, L. Martín-Moreno, and J. B. Pendry, "Surfaces with holes in them: New plasmonic metamaterials," *J. Opt. A, Pure Appl. Opt.*, vol. 7, no. 2, p. S97, 2005. [Online]. Available: http://stacks.iop.org/1464-4258/7/i=2/a=013
[45] D. Pozar, *Microwave Engineering*, 4th ed. Hoboken, NJ, USA: Wiley, 2011. [Online]. Available: https://books.google.se/books?id=JegbAAAAQBAJ
[46] V. Galdi and I. M. Pinto, "A simple algorithm for accurate location of leaky-wave poles for grounded inhomogeneous dielectric slabs," *Microw. Opt. Technol. Lett.*, vol. 24, no. 2, pp. 135–140, 2000.

FATEMEH GHASEMIFARD (GS'11) received the B.Sc. degree in electrical engineering from the Iran University of Science and Technology, Tehran, Iran, and the M.Sc. degree in electromagnetics engineering from the University of Tehran, Tehran, Iran, in 2011. She is currently pursuing the Ph.D. degree with the KTH Royal Institute of Technology, Stockholm, Sweden. Her current research interests include metamaterials, metasurfaces, higher-symmetric periodic structures, and analytical and numerical methods in electromagnetics. In 2013, she was a recipient of the Program of Excellence Award offered by the Electrical Engineering School, KTH Royal Institute of Technology.

MARTIN NORGREN received the M.Sc. and Ph.D. degrees from the KTH Royal Institute of Technology, in 1992 and 1997, respectively. He is currently a Professor in electromagnetic theory with the KTH Royal Institute of Technology. His research interest is electromagnetic theory in general, with particular interests in waveguide problems, inverse problems, and inverse source problems.

OSCAR QUEVEDO-TERUEL (M'10–SM'17) received the degree in telecommunication engineering from the Carlos III University of Madrid, Madrid, Spain, in 2005, a part of which was done at the Chalmers University of Technology, Gothenburg, Sweden, and the Ph.D. degree from the Carlos III University of Madrid in 2010. He was invited as a Post-Doctoral Researcher at the Delft University of Technology, Delft, The Netherlands. From 2010 to 2011, he was a Research Fellow with the Department of Theoretical Physics of Condensed Matter, Autonomous University of Madrid, Madrid. He was a Post-Doctoral Researcher at the Queen Mary University of London, London, U.K., from 2011 to 2013.

In 2014, he joined the School of Electrical Engineering, KTH Royal Institute of Technology, Stockholm, Sweden, where he is currently an Associate Professor and the Director of the Master's Program in electromagnetics, fusion, and space engineering. He has been an Associate Editor of the IEEE TRANSACTIONS ON ANTENNAS AND PROPAGATION since 2018, and he is the delegate of EurAAP for Sweden, Norway, and Iceland for the period 2018–2020. He is a Distinguished Lecturer of the IEEE Antennas and Propagation Society for the period 2019–2021.

He has made scientific contributions in microstrip patch antennas, lens antennas, metasurfaces, higher symmetries, transformation optics, and high-impedance surfaces. He has co-authored over 60 papers in international journals and over 120 at international conferences, and has received approval on two patents.

GUIDO VALERIO (S'06–M'10–SM'18) received the M.S. degree *(cum laude)* in electronic engineering and the Ph.D. degree in electromagnetics from La Sapienza University, Rome, Italy, in 2005 and 2009, respectively. In 2008, he was a Visiting Scholar at the University of Houston, TX, USA. From 2011 to 2014, he was a Researcher at the Institute d'Électronique et de Télécommunications de Rennes, France. Since 2014, he has been an Associate Professor with the Laboratoire d'Électronique and Électromagnétisme, Sorbonne Université, Paris, France.

His scientific interests involve antenna design and numerical methods for wave propagation and scattering in complex structures, namely, periodic Green's function computation, modal properties of multilayered structures, full-wave methods for SIW, and modeling of periodic structures with higher-symmetries.

In 2008, he was a recipient of the Leopold B. Felsen Award for Excellence in Electrodynamics. In 2009, he was a finalist for the Young Engineering Prize at the European Microwave Conference. In 2010, he was a recipient of the Barzilai Prize for the best paper at the National Italian Congress of Electromagnetism (XVIII RiNEm). In 2014, he was a recipient of the RMTG Award for junior researchers presented at the IEEE Antennas and Propagation Society Symposium, Memphis, TN, USA. In 2018, he was a co-author of the best paper in Electromagnetic and Antenna theory at the 12th European Conference on Antennas and Propagation, London, U.K.